Respiratory Effects and Systemic Stress Response Following Acute Acrolein Inhalation in Rats

Samantha J. Snow,[*,1] Marie A. McGee,[†] Andres Henriquez,[‡] Judy E. Richards,[*] Mette C. Schladweiler,[*] Allen D. Ledbetter,[*] and Urmila P. Kodavanti[*,‡]

[*]Environmental Public Health Division, NHEERL, US Environmental Protection Agency, Durham, North Carolina; [†]Oak Ridge Institute for Science and Education, Durham, North Carolina; and [‡]Curriculum in Toxicology, University of North Carolina at Chapel Hill, Chapel Hill, North Carolina

[1]To whom correspondence should be addressed at Environmental Public Health Division, NHEERL, US Environmental Protection Agency, 109 T.W. Alexander Dr., Durham, NC 27711. Fax: (919) 541-0026. E-mail: snow.samantha@epa.gov.

ABSTRACT

Previous studies have demonstrated that exposure to the pulmonary irritant ozone causes myriad systemic metabolic and pulmonary effects attributed to sympathetic and hypothalamus-pituitary-adrenal (HPA) axis activation, which are exacerbated in metabolically impaired models. We examined respiratory and systemic effects following exposure to a sensory irritant acrolein to elucidate the systemic and pulmonary consequences in healthy and diabetic rat models. Male Wistar and Goto Kakizaki (GK) rats, a nonobese type II diabetic Wistar-derived model, were exposed by inhalation to 0, 2, or 4 ppm acrolein, 4 h/d for 1 or 2 days. Exposure at 4 ppm significantly increased pulmonary and nasal inflammation in both strains with vascular protein leakage occurring only in the nose. Acrolein exposure (4 ppm) also caused metabolic impairment by inducing hyperglycemia and glucose intolerance (GK > Wistar). Serum total cholesterol (GKs only), low-density lipoprotein (LDL) cholesterol (both strains), and free fatty acids (GK > Wistar) levels increased; however, no acrolein-induced changes were noted in branched-chain amino acid or insulin levels. These responses corresponded with a significant increase in corticosterone and modest but insignificant increases in adrenaline in both strains, suggesting activation of the HPA axis. Collectively, these data demonstrate that acrolein exposure has a profound effect on nasal and pulmonary inflammation, as well as glucose and lipid metabolism, with the systemic effects exacerbated in the metabolically impaired GKs. These results are similar to ozone-induced responses with the exception of lung protein leakage and ability to alter branched-chain amino acid and insulin levels, suggesting some differences in neuroendocrine regulation of these two air pollutants.

Key words: acrolein; stress response; neuroendocrine; nasal injury; pulmonary injury.

Differential water solubility and chemistry of inhaled pollutants influences their deposition site along the nasal, tracheobronchial, and pulmonary airways. Sensory irritants such as acrolein, ammonia, and sulfur dioxide, with high water solubility, have been shown to primarily deposit in the nasal passages of rodents while pulmonary irritants such as phosgene, ozone, and nitrogen dioxide, which are less water soluble, deposit primarily in the lower airways and pulmonary structures (U.S. EPA, 2013). The deposition sites for these air pollutants often overlap depending on animal species, exposure concentration, and duration of exposure (Alarie, 1973). The neural pathways stimulated by these toxicants differ substantially based on their deposition site, leading to differential airway and cardiac reflex responses. The integration of sensory signals results in efferent flow through phrenic, vagus, and splanchnic nerves to induce these reflexes (Alarie, 1973).

Acrolein, a sensory irritant, induces respiratory and cardiovascular reflex reactions through the trigeminal nerve upon inhalation (Alarie, 1973), whereas ozone, a pulmonary irritant, stimulates reflex cardiopulmonary changes through activation of myelinated nerves and nonmyelinated vagal sensory C-fibers (Mazzone and Undem, 2016). Relatively little is known about the

central nervous system integration of signals generated in the trigeminal ganglion and its overlap between the central areas that receive signals from the vagus nerve through jugular and nodose ganglia.

Acrolein, a chemically simple but highly reactive unsaturated aldehyde, is produced and released during organic combustion processes, photochemical reactions of volatile organic components in the air, and endogenously as a byproduct of lipid peroxidation. Acrolein can form adducts with biomolecules (Moghe et al., 2015) and is associated with increased risk of cardiovascular disease (DeJarnett et al., 2014). Although ambient environmental concentrations of acrolein are present in the low ppb range, levels can vary reaching as high as 50 ppm in mainstream cigarette smoke and 60 ppm in combustion smoke (Einhorn, 1975; Struve et al., 2008). Reflex cardiopulmonary responses triggered by inhaled acrolein include bradycardia, decreased breathing frequency due to prolonged expiratory time, and increased vasoconstriction/systemic blood pressure (Alarie, 1973). Sympathetic and parasympathetic pathways have been postulated to be involved in nasal and pulmonary effects of acrolein (Bosse, 2014; Delaunois et al., 1997).

A number of studies have shown that acute inhalation ozone, induces ventilatory changes, and activates stress responsive regions in the brain (Chounlamountry et al., 2015; Gackiere et al., 2011; Soulage et al., 2004; Taylor-Clark and Undem, 2011). We have recently shown that acute inhalation of ozone produces bradycardia, hypothermia (Gordon et al., 2014), tachypnea (Snow et al., 2016), and myriad systemic metabolic and pulmonary effects that are attributed to the activation of the sympathetic nervous system and hypothalamus-pituitary-adrenal (HPA)-axis (Bass et al., 2013; Miller et al., 2015, 2016b). Ozone-induced systemic metabolic and pulmonary injury/inflammation-related effects are markedly diminished in adrenalectomized and demedullated rats, suggesting a central role for sympathetic- and HPA-stimulated increases in stress hormones (Miller et al., 2016c). However, if acrolein may also induce systemic metabolic effects and how it may relate to respiratory toxicity is poorly understood.

In this study, we examined nasal, pulmonary, and systemic effects of acrolein in rats acutely exposed to a range of concentrations to allow us to better understand the systemic consequences and respiratory effects of acute acrolein inhalation with special emphasis to the relation between respiratory effects and systemic hormonal and metabolic changes. Furthermore, exposures to particulate and gaseous air pollutants have been linked to diabetes (Thiering and Heinrich, 2015), but the mechanisms remain elusive. Since acute ozone exposure causes an array of metabolic effects in healthy rats including impaired insulin secretion (Kodavanti, 2016), in this study, we explored risk factors that might contribute to exacerbated systemic metabolic and respiratory responses following an acute acrolein inhalation in healthy Wistar as well as Goto Kakizaki (GK) rats, a Wistar-derived strain that is genetically predisposed to nonobese type 2 diabetes.

MATERIALS AND METHODS

Animals. Adult (10-weeks old) male Wistar (362.9 ± 4.7 g) and GK (249.8 ± 2.2 g) rats were obtained from Charles Rivers Laboratories (Raleigh, North Carolina) and maintained in a specific pathogen free AAALAC-approved animal facility on a 12-h light/dark cycle. Animals were housed 2 per cage by strain in polycarbonate cages with beta chip bedding. They received food (Rodent Chow 5001: Ralston Purina Laboratories, St Louis,

Missouri) and water *ad libitum*. All experimental protocols were approved by the U.S. EPA's Institutional Animal Care and Use Committee.

Acrolein exposures. Prior to exposure, all animals were acclimated to the nose-only exposure tubes (Lab Products, Seaford, Delaware) for 2 consecutive days for 1 and 2 h, respectively. Following acclimation, animals were exposed to either 0, 2, or 4 ppm acrolein for 4 h/d for 1 day or 2 consecutive days (n = 6/group). Acrolein gas from a 1000 ppm cylinder was diluted with filtered compressed air (supplied by a medical grade air compressor) to achieve the desired final concentrations. Chamber pressure and flow rates of the compressed air (10 L/min) and acrolein were monitored throughout the exposures. Chamber concentrations were determined by taking syringe samples via an unused animal port and injected into a HP5580 gas chromatograph (GMI Inc., Ramsey, Minnesota). Flows were adjusted as necessary to maintain the targeted acrolein concentrations of 0, 2 (1.97 ± 0.14), and 4 (4.00 ± 0.14) ppm. Temperature (21.8°C ± 0.3°C) and relative humidity (38.9% ± 2.7%) in the room where the nose-only chambers were located were monitored approximately once per hour during exposure.

Whole-body plethysmography. Breathing parameters were measured using whole-body plethysmography (EMKA Technologies, Paris, France) in unanesthetized, unrestrained rats. Measurements were taken from only the 2-day group on 3 separate occasions at the same time of the day: pre-exposure (baseline), immediately following the first exposure before glucose tolerance testing (GTT), and immediately following the second exposure before necropsy. The animals were acclimated to the plethysmography chambers for 1 min before a 5 min assessment of a variety of ventilatory parameters including inspiratory time (T_i), expiratory time (T_e), enhanced pause (PenH), breathing frequency, tidal volume, and minute volume.

Glucose tolerance test. GTT was performed only on the 2-day group following the first day of exposure to acrolein as previously described in Miller et al. (2015) with some minor alterations. Briefly, rats were fasted for approximately 6 h prior to testing. Baseline glucose levels were measured via a tail prick prior to I.P. injection of glucose (1 g/5 ml/kg of a 20% D-glucose solution in saline). Blood glucose measurements were made every 30-min postinjection for the next 120 min for a total of 5 readings.

Necropsy and sample collection. Rats were euthanized within 1 h following a 1 or 2 day acrolein exposure with an overdose of sodium pentobarbital (Fatal-Plus diluted 1:1 with saline; > 200 mg/kg; I.P. Vortech Pharmaceuticals, Ltd., Dearborn, Michigan). Blood samples were collected from the abdominal aorta for serum and plasma. The right lung was lavaged and bronchoalveolar lavage fluid (BALF) was processed as previously described (Snow et al., 2016). Following BALF collection, the rat was decapitated and the lower jaw was removed. The nasopharyngeal passage was cannulated and the nasal cavity was lavaged using Ca^{2+}/Mg^{2+} free phosphate buffered saline (2 ml/rat, pH 7.4, 37 °C).

BALF and nasal lavage fluid analysis. Aliquots of BALF and nasal lavage fluid (NALF) were used to determine total cell counts with a Z1 Beckman-Coulter Counter (Beckman-Coulter, Inc., Miami, Florida). Cell differentials for BALF were conducted as previously described (Snow et al., 2014). For NALF, an aliquot
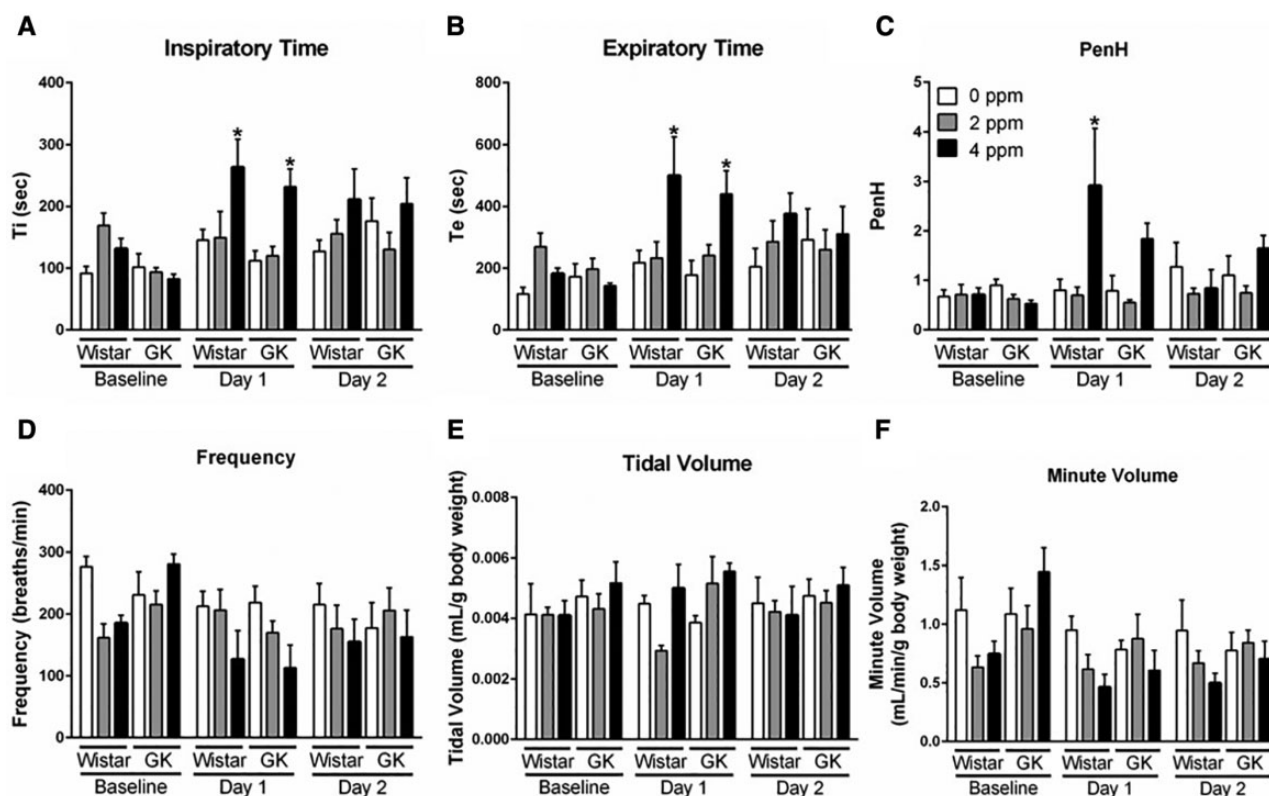
Figure 1. Exposure to acrolein alters breathing parameters. Whole-body plethysmography was performed on Wistar and GK rats following exposure to 0, 2, or 4 ppm acrolein. Measurements for (A) inspiratory time, (B) expiratory time, (C) PenH, (D) frequency, (E) tidal volume, and (F) minute volume were taken from only the 2-day group on 3 separate occasions at the same time of the day at baseline prior to exposure, and immediately following exposure on Days 1 and 2. Data show mean ± SE (n = 6/group). *$p < .05$ significantly different than 0 ppm group within same strain.

was centrifuged (Shandon 3 Cytospin, Shandon, Pittsburgh, Pennysylvania) and stained with Leukostat (Fisher Scientific, Pittsburgh, Pennsylvania) to prepare cell differential slides. Images of NALF stained slides were taken using a Nikon Eclipse Diaphot 300 microscope (Nikon Metrology Inc., Brighton, Michigan) and Sony DXC970MD-3CCD color video camera (Tokyo, Japan) at 40× magnification. Cell-free BALF and NALF were analyzed for markers of lung injury including total protein, albumin, N-acetyl-β-D-glucosaminidase (NAG) activity, γ-glutamyl transferase (GGT) activity, and lactate dehydrogenase (LDH) activity as previously described (Snow et al., 2014).

Serum and plasma analysis. An aliquot of EDTA plasma was used to determine complete blood counts (CBCs) using a Beckman-Coulter AcT blood analyzer (Beckman-Coulter Inc., Miami, Florida). A separate aliquot of EDTA was used for analysis of the catecholamines adrenaline and noradrenaline, as well as corticosterone as previously described (Miller et al., 2016b). Serum aliquots were used to measure metabolic markers (total cholesterol, LDL cholesterol, HDL cholesterol, triglycerides, branched-chain amino acids [BCAA], free fatty acids [FFA], and insulin) as previously described in Miller et al. (2016b).

Statistical analysis. All statistical analyses were conducted using GraphPad Prism v6.0 software (San Diego, California). The plethysmography and GTT data were analyzed using a repeated measures 2-way ANOVA. GTT data were first normalized to average Wistar 0 ppm, 0 min blood glucose levels and analyzed for area under the curve by the trapezoidal method. All other data were analyzed at each time point using a 2-way ANOVA

with strain and exposure as factors. The Holm-Sidak's *post-hoc* test was used to correct for all multiple comparisons. A *p*-value < .05 was considered statistically significant.

RESULTS

Acrolein Alters Breathing Parameters Following Exposure

Respiratory parameters were measured using whole-body plethysmography to determine if pulmonary parameters in Wistar and GK rats were altered immediately following a 2 and 4 ppm acrolein exposure for 4 h. Both T_i and T_e were significantly increased in both strains only after the first exposure to 4 ppm acrolein (Figs. 1A and 1B). Acrolein exposure (4 ppm) on Day 1 also increased PenH levels (Figure 1C), an unitless marker for labored breathing that is calculated using T_e as one of its factors (Hamelmann et al., 1997). No significant changes were noted in the levels of T_i, T_e, and PenH after the second day of exposure regardless of acrolein concentration. Although not significant, there was a clear decrease in frequency (Figure 1D). When normalized to body weight, the minute volume in Wistars tended to be lower at 4 ppm acrolein at both time points (Figure 4F). No changes were noted in tidal volume (Figure 1E).

Exposure to Acrolein Leads to Increased Nasal and Pulmonary Injury

Overall, acrolein exposure caused noticeably more damage in the nasal passages as opposed to the lung as determined by analysis of injury markers (Figure 2). This included significant elevations in levels of NALF total protein (Figure 2B) and albumin (Figure 2D), markers of vascular permeability; NAG activity
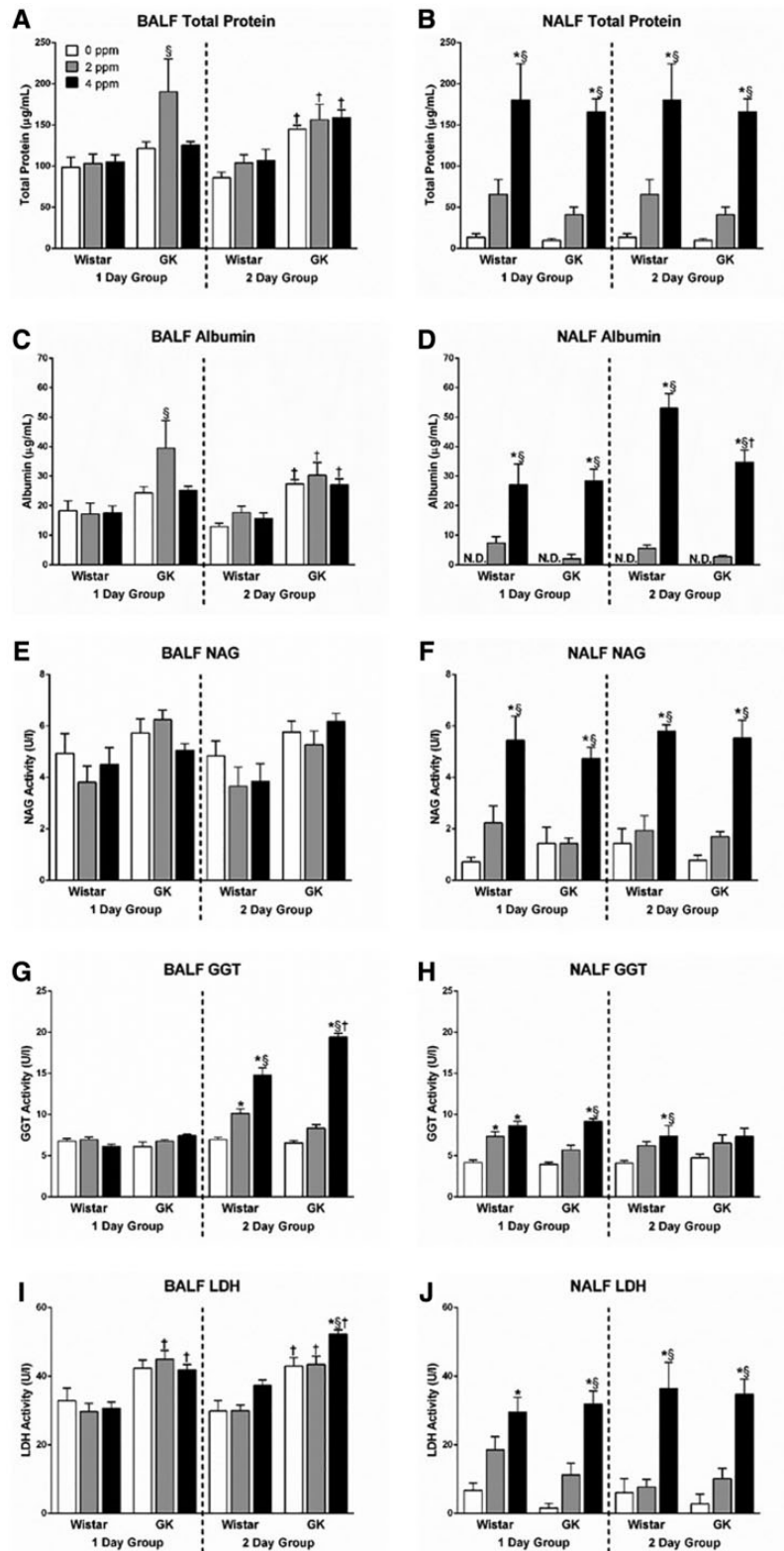
Figure 2. Acrolein exposure increases biomarkers of pulmonary and nasal injury. BALF (left column) and NALF (right column) samples were collected at necropsy following either 1 or 2 days of exposure in Wistar and GK rats exposed to 0, 2, or 4 ppm acrolein. Samples were analyzed for (**A** and **B**) total protein, (**C** and **D**) albumin, (**E** and **F**) NAG activity, (**G** and **H**) GGT activity, and (**I** and **J**) LDH activity. Data show mean ± SE (n = 6/group). *$p < .05$ significantly different than 0 ppm group within same strain. §$p < .05$ significantly different than 2 ppm group within same strain. †$p < .05$ significantly different between strains at the same dose. N.D., not detectable.
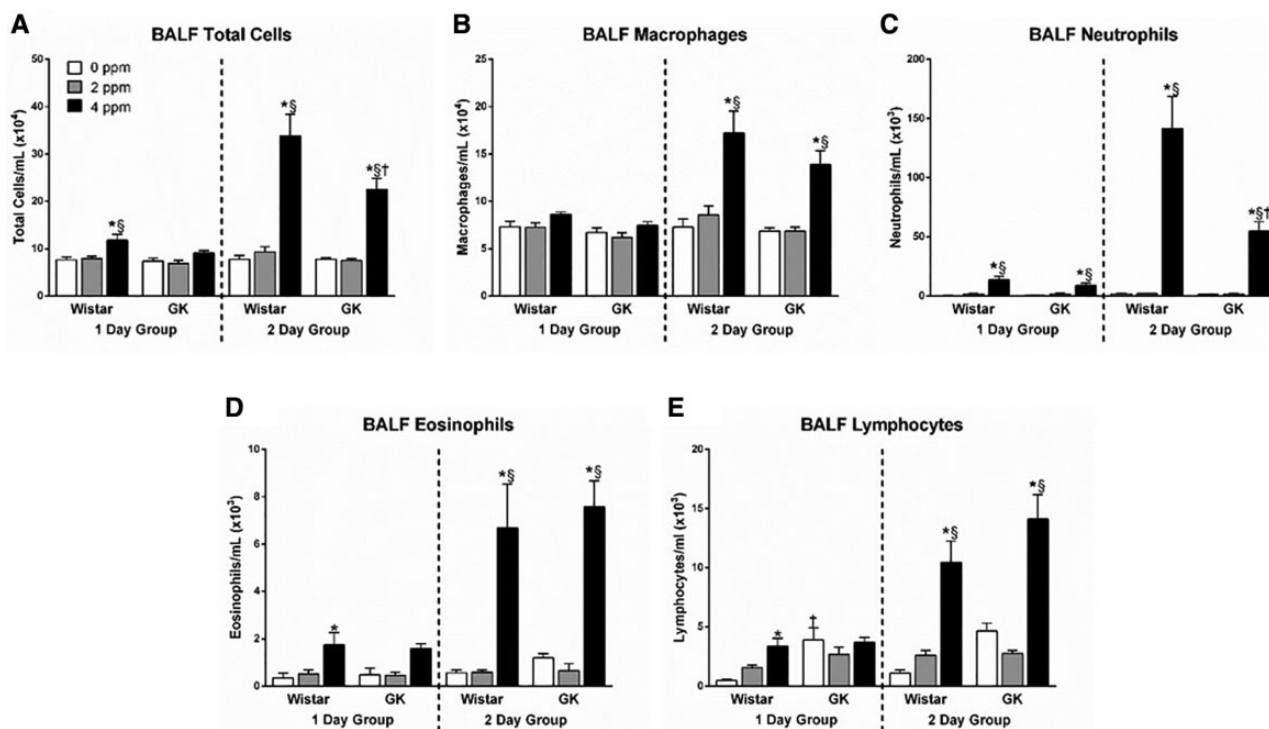
Figure 3. Inflammatory cells are increased in BALF following acrolein exposure. BALF samples collected at necropsy following either 1 or 2 days of exposure in Wistar and GK rats exposed to 0, 2, or 4 ppm acrolein were analyzed for (A) total cells, (B) macrophages, (C) neutrophils, (D) eosinophils, and (E) lymphocytes. Data show mean ± SE (n = 6/group). *$p < .05$ significantly different than 0 ppm group within same strain. §$p < .05$ significantly different than 2 ppm group within same strain. †$p < .05$ significantly different between strains at the same dose.

(Figure 2F), a marker for macrophage activation; as well as GGT activity (Figure 2H) and LDH activity (Figure 2J), markers of cellular injury. Increases in the levels of the NALF markers were immediate and occurred in both the 1- and 2-day groups. Although the high dose of acrolein consistently increased levels of these nasal injury biomarkers, the trends in elevations were also evident with the 2 ppm concentration (Figure 2). No strain-related differences were noted at baseline (air controls) or after acrolein exposure in NALF injury markers.

In contrast to the NALF findings, there were strain-related differences in the baseline levels of BALF injury markers as the GKs expressed higher levels of BALF total protein (Figure 2A), albumin (Figure 2C), and LDH activity (Figure 2I) compared with the Wistars. Furthermore, in stark contrast to the injury present in the NALF, exposure to acrolein only led to significant increases in BALF GGT activity (Figure 2G) and LDH activity (Figure 2I) without significant increases in protein and albumin leakage. The effect on lung cell injury markers occurred maximally in the 2-day group.

Pulmonary and Nasal Inflammation Are Exacerbated Following Acrolein Exposure

Exposure to 4 ppm acrolein led to significant increases in BALF total cells in both strains (Figure 3A), indicating acrolein-induced lung inflammation. This effect was slight but apparent in the 1-day group and exacerbated following the second acrolein exposure (Figure 3). The cellular increase present in the BALF was driven by the influx of a variety of inflammatory cells including macrophages (Figure 3B), neutrophils (Figure 3C), eosinophils (Figure 3D), and lymphocytes (Figure 3E). There was also a significant difference between the strains for the total number

of cells (Figure 3A) that was solely driven by the elevated neutrophilic inflammation (Figure 3C) present in the Wistars.

NALF total cells were also significantly elevated in both strains following exposure to 4 ppm acrolein exposure (Figure 4A). There was a trend for this effect to occur in the 1-day group and was clearly evident in the 2-day group (Figure 4). Due to several factors including the scarcity of cells to count on the air control slides, the occurrence of numerous unidentifiable lysed cells, and the presence of epithelial cells, we choose to not perform cell differentials on the slides obtained from the NALF samples. Instead, representative images are depicted (Figure 4B). These images clearly illustrate an increase in total cell number and neutrophilic inflammation with the rise in acrolein dose regardless of strain, leading to the presence of suppurative inflammation in the 2-day group following exposure to 4 ppm acrolein.

In addition to the pulmonary and nasal inflammation, a CBC was performed to examine systemic inflammation by measuring circulating white blood cells (WBCs) and lymphocyte numbers (Table 1). There were no statistically significant differences in circulating WBC or lymphocytes following exposure to acrolein when using a 2-way ANOVA or Pearson's correlation. However, when using a Student's t-test to compare 4 ppm acrolein exposures to filtered air for each strain and time point, there were significant increases in WBC (GK 2-day group, $p = .0168$) and significant decreases in circulating lymphocytes (Wistar 1-day group, $p = .0041$).

Circulating Stress Hormone Levels Are Altered by Acrolein Exposure

Previous studies from our lab have demonstrated elevations in circulating adrenaline (Miller et al., 2016b) and corticosterone (Miller et al., 2016a) levels following acute ozone exposures. To determine if exposure to acrolein also resulted in the elevation
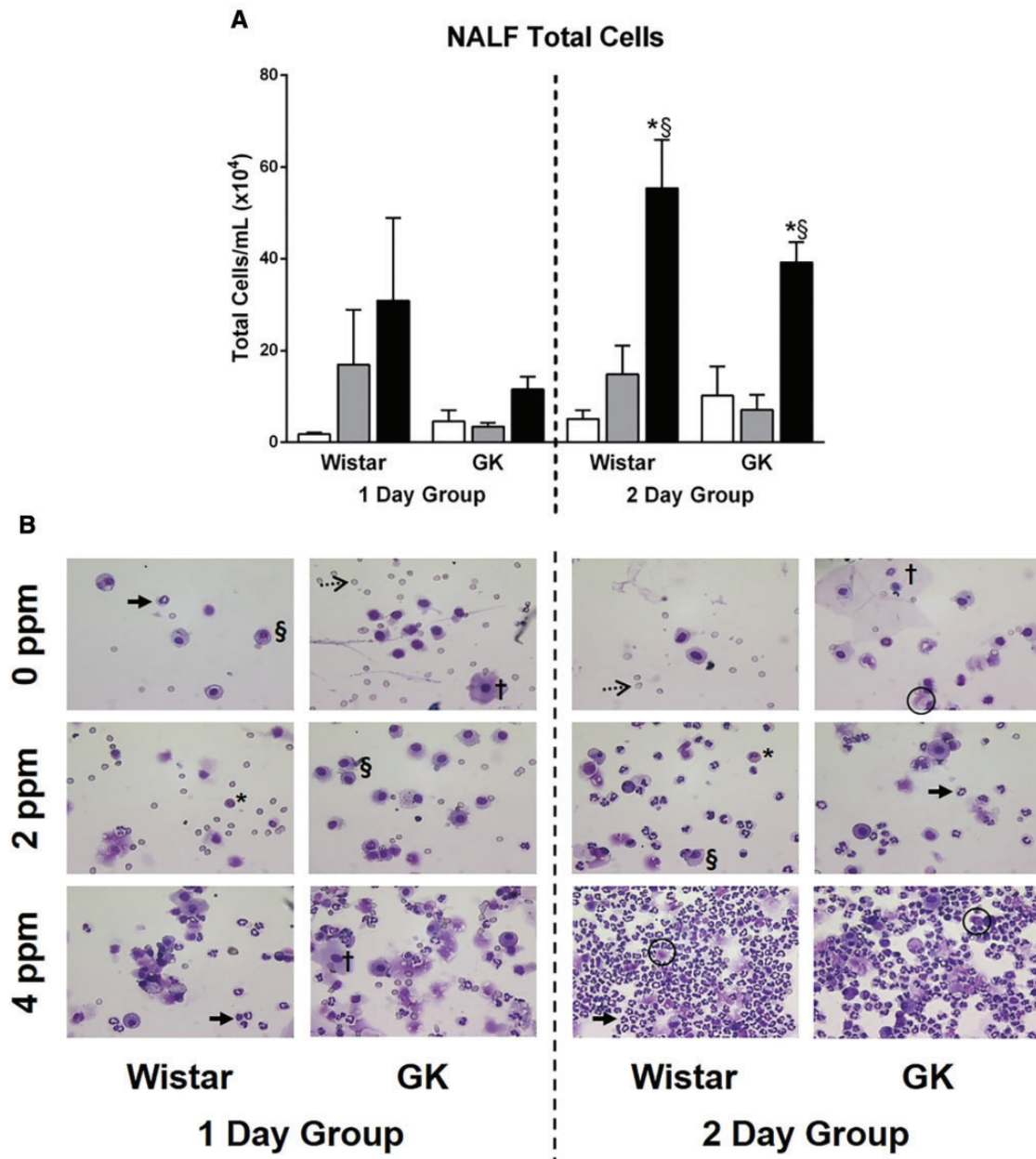
Figure 4. Acrolein leads to influx of inflammatory cells in nasal passages following exposure. NALF samples collected at necropsy were analyzed following either 1 or 2 days of exposure to 0, 2, or 4 ppm acrolein in Wistar and GK rats. A, Total cells were measured using a cell counter. Data show mean ± SE (n = 6/group). *p < .05 significantly different than 0 ppm group within same strain. §p < .05 significantly different than 2 ppm group within same strain. B, Representative images from stained slides demonstrate the presence of epithelial cells (squamous (†) and ciliated (O)), inflammatory cells (neutrophils (→), macrophages (§), and eosinophils (*)), and erythrocytes (····>) in the NALF following exposure.

of these stress hormones, we measured circulating levels of adrenaline, noradrenaline, and corticosterone following a 1- or 2-day exposure to acrolein. There was no significant effect on serum adrenaline levels due to exposure; however, levels in the GK 0 ppm group were significantly higher than the Wistars at the same dose at 1 day (Figure 5A). No changes were noted in noradrenaline levels following acrolein exposure regardless of dose, strain, or time point (Figure 5B). Serum corticosterone levels were significantly elevated in both the Wistars and GKs in the 1-day group after exposure to 4 ppm acrolein, and approached significance (p = .084) in the Wistar 2-day group (Figure 5C).

Acrolein Exposure Leads to Hyperglycemia and Glucose Intolerance
GTT was performed in the 2-day group following the first day of exposure to determine if acrolein induced metabolic impairment (Figure 6A). At all time points tested, the nonobese type 2 diabetic GK animals had significantly higher blood glucose levels regardless of exposure dose as expected. Prior to exogenous glucose injection (0 min), blood glucose levels were significantly elevated in the GKs exposed to acrolein but not the Wistars, indicating acrolein-induced hyperglycemia. Furthermore, exposure to 4 ppm acrolein induced glucose intolerance in both the GK and Wistar rats as indicated by the inability of blood glucose levels to return to baseline over time. This response was

exacerbated in the GKs compared with the Wistars as demonstrated by the increase in area under the curve (Figure 6B). Acrolein exposure did not alter serum insulin levels or HOMA-IR regardless of dose, time point, or strain (data not shown). HOMA-β values, which indicate β-cell function, were significantly lower in the GK model regardless of acrolein dose or time point, confirming the model's diabetic status (HOMA-β: Wistar air group, 23.84 ± 3.34; GK air group, 7.30 ± 1.34; mean ± SEM).

Serum Metabolic Markers Are Increased Following Acrolein Exposure

We have previously demonstrated ozone-induced increases in cholesterol, FFA, triglycerides, and BCAA (Miller *et al.*, 2015, 2016c) and wanted to determine if these same metabolic effects are present following an acute acrolein exposure. A 2-day exposure to 4 ppm acrolein led to significant increases in total cholesterol in GK rats (Figure 7A) and in LDL cholesterol (Figure 7B) in both strains. No acrolein-induced changes were noted in HDL cholesterol levels; however, both total and HDL cholesterol were elevated at baseline in GKs as compared with Wistars (Figs. 7A and 7C). FFA were significantly elevated in Wistars following a 1 day 4 ppm acrolein exposure, with levels further exacerbated in the GKs (Figure 7D). FFA levels returned to baseline in the 2-day group for both strains demonstrating an adaptive response. Acrolein exposure led to slight elevations in

Table 1. Circulating WBC and Lymphocyte Counts in Wistars and GKs Following Exposure to Acrolein for 1 or 2 Days

Exposure Duration	Strain	Acrolein (ppm)	WBC ($\times 10^6$/ml)	Lymphocytes ($\times 10^6$/ml)
1 day	Wistar	0	5.50 ± 0.38	4.23 ± 0.28
		2	6.68 ± 1.05	4.37 ± 0.91
		4	7.12 ± 0.71	2.95 ± 0.20
	GK	0	7.70 ± 0.79	5.62 ± 0.67
		2	8.25 ± 0.95	5.83 ± 0.67
		4	9.35 ± 0.33	4.17 ± 0.13
2 days	Wistar	0	6.45 ± 0.84	4.48 ± 0.61
		2	6.30 ± 0.83	4.75 ± 0.58
		4	8.80 ± 1.08	4.00 ± 0.60
	GK	0	6.66 ± 1.26	4.92 ± 0.80
		2	7.82 ± 1.15	5.62 ± 0.79
		4	10.52 ± 0.47	4.05 ± 0.36

Data are mean ± SE (n = 6/group) measured in EDTA plasma. WBC, white blood cells; GK, Goto Kakizaki.

triglyceride levels in both strains following a 1-day exposure similar to the response seen in FFA; however, this was not statistically significant (Figure 7E). Neither acrolein dose, time point, nor strain led to changes in serum BCAA levels (Figure 7F).

DISCUSSION

Acute acrolein inhalation induced nasal and pulmonary neutrophilic inflammation whereas vascular protein leakage occurred only in the nose. Circulating adrenaline levels were only slightly increased with acrolein, while significant increases in corticosterone were evident in both strains immediately following the first exposure. Metabolically, acrolein-induced hyperglycemia and glucose intolerance (GK > Wistar), and increases in total cholesterol, (GKs only), LDL cholesterol (both strains), and FFA (GK > Wistar) which were similar to our previous findings with ozone (Miller *et al.*, 2015, 2016c). However, no increases in BCAA or decreases in insulin levels were evident in either strain after acrolein exposure. These data suggest that while systemic changes associated with glucose and lipid metabolic alterations following acrolein exposure are similar to that of ozone (Miller *et al.*, 2015), exposure to these different irritants results in some divergence in neuroendocrine responsiveness.

Acrolein inhalation is known to reduce respiratory rate and minute volume as demonstrated here by prolonging expiration, which is thought to be a protective reflex mechanism to reduce the dose to the lower airways and alveoli (Lee *et al.*, 1992; Perez *et al.*, 2015). Breathing parameters were not monitored during inhalation; however, when determined immediately postexposure, both inhalation and exhalation phases were prolonged with concomitant increases in PenH, suggesting labored breathing. These changes in plethysmography measures with acrolein likely resulted from nasal injury stemming from its predominant deposition in the nasal airways.

Acrolein deposits primarily in the complex nasal airways of rodents and induces nasal injury and inflammation (Morris *et al.*, 1999; Struve *et al.*, 2008). Despite increased cellular injury markers in both nasal and pulmonary lavage fluids following acrolein exposure, the stark differences in vascular protein leakage between the nose and lung illustrates the role of deposition differences along the airways. Our data demonstrate that the vascular protein leakage might be caused by capillary pressure changes and cell injury in the nose, suggesting increased local vascular permeability (Conklin, 2016). This is in contrast to previously reported lung protein leakage following ozone exposure, which might induce changes in pulmonary microvasculature
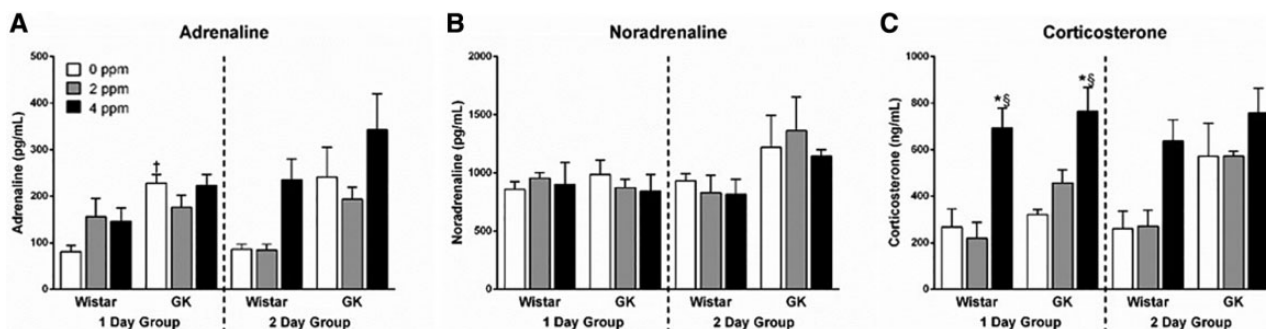

Figure 5. Exposure to acrolein increases corticosterone levels. Stress hormones including (**A**) adrenaline, (**B**) noradrenaline, and (**C**) corticosterone were measured in EDTA plasma samples in Wistar and GK rats exposed to 0, 2, or 4 ppm acrolein for 1 or 2 days. Data show mean ± SE (n = 6/group). *$p < .05$ significantly different than 0 ppm group within same strain. §$p < .05$ significantly different than 2 ppm group within same strain. †$p < .05$ significantly different between strains at the same dose.
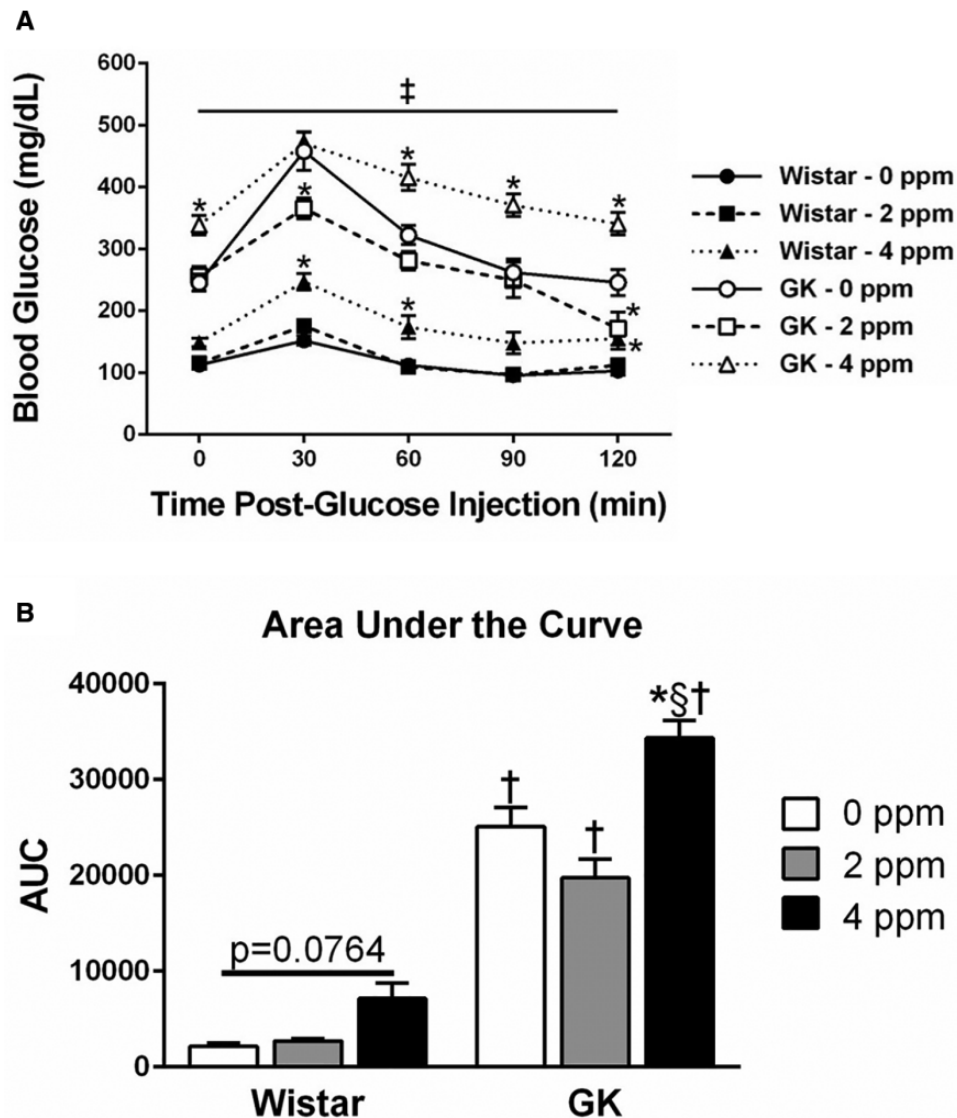
Figure 6. Acrolein exposure induces hyperglycemia and glucose intolerance. **A,** GTT was conducted in Wistar and GK rats exposed to 0, 2, or 4 ppm acrolein for 1 day. **B,** AUC, normalized to the average Wistar 0 ppm, 0 min blood glucose levels, were calculated for each group. Data show mean ± SE (n = 6/group). [‡]$p < .05$ significantly different between strains at the same dose. [‡]$p < .05$ significantly different between strains at all doses. [*]$p < .05$ significantly different than 0 ppm group within same strain. [§]$p < .05$ significantly different than 2 ppm group within same strain. [†]$p < .05$ significantly different between strains at the same dose.

(Miller *et al.*, 1978). Acrolein induces systemic vasoconstriction as opposed to ozone that induces vasodilation (Perez *et al.*, 2015; Wagner *et al.*, 2014); however, the differences in pulmonary microcirculation might be distinct from peripheral vessels. It is also likely that some deposition of acrolein, particularly at the high concentration, into the lower airways led to increases in cell injury markers such as GGT and LDH but did not cause vascular leakage.

Marked increases in NALF neutrophils after acrolein exposure is consistent with previous studies (Dorman *et al.*, 2008). However, it was surprising to note that acrolein, despite causing no lung protein leakage, produced a robust pulmonary neutrophilic inflammation response, in addition to increases in eosinophils and lymphocytes. Given that acrolein caused marked increases in corticosterone but only small increases in adrenaline, it is possible that corticosterone may have contributed to the neutrophilic inflammation caused by HPA-activation after

exposure since the egress and extravasation of immune cells are tightly regulated by circulating stress hormones (Dhabhar *et al.*, 2012). Although the data were insignificant, there was a small decrease in circulating lymphocytes despite a small increase in total WBCs after the first acrolein exposure, which might suggest cell-specific extravasation of neutrophils and lymphocytes to the nose and pulmonary tissue, modulated by the changes in stress hormones.

Acrolein exposure induced a robust increase in corticosterone and only a small increase in adrenaline levels, as opposed to ozone exposure, which increased both stress hormones (Miller *et al.*, 2015, 2016c). This difference may in part stem from the differences in nerve reflexes initiated with acrolein likely preferentially triggering activation of the nasal trigeminal nerve while ozone has been linked to pulmonary C-fiber-mediated central activation (Taylor-Clark and Undem, 2010). Since our previous ozone studies were conducted in the WKY rat model,
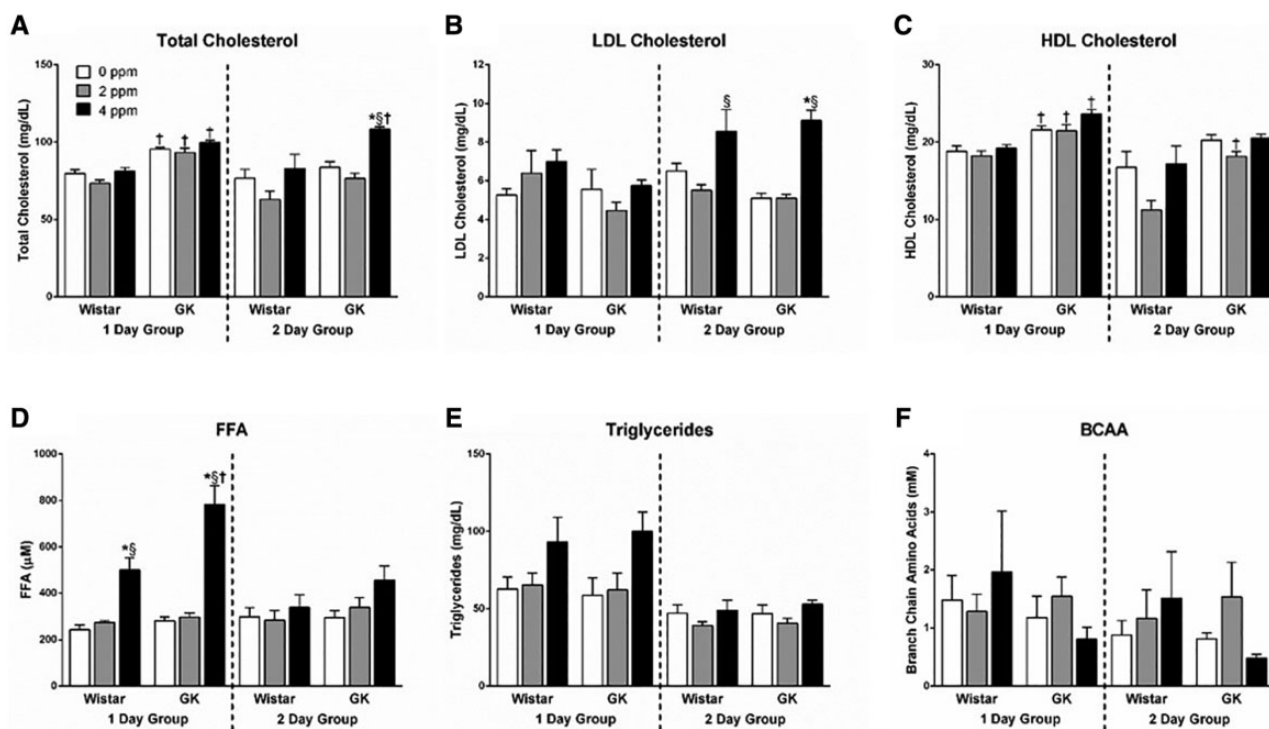
Figure 7. Serum metabolic markers increased after acrolein exposure. Metabolic markers including (**A**) total cholesterol, (**B**) LDL cholesterol, (**C**) HDL cholesterol, (**D**) FFA, (**E**) triglycerides, and (**F**) BCAA were measured in serum samples in Wistar and GK rats exposed to 0, 2, or 4 ppm acrolein for 1 or 2 days. Data show mean ± SE (n = 6/group). *$p < .05$ significantly different than 0 ppm group within same strain. §$p < .05$ significantly different than 2 ppm group within same strain. †$p < 0.05$ significantly different between strains at the same dose.

one can presume that the difference in the stress hormone increases after acrolein and ozone exposure might also relate to differences between these rat strains.

Exposure to inhaled particulate matter and gaseous pollutants has been linked to acceleration of cardiovascular and metabolic diseases such as diabetes (Kodavanti, 2015; Munzel et al., 2016). We have previously demonstrated that acute ozone exposure through activation of sympathetic nervous system and the HPA-axis induces hyperglycemia and glucose intolerance through increased hepatic gluconeogenesis and impairment of glucose-mediated beta cell insulin secretion (Miller et al., 2016b). Similar to ozone (Bass et al., 2013; Miller et al., 2015, 2016b,c), acrolein also induced hyperglycemia and glucose intolerance, especially in GK rats, yet there was no effect on circulating insulin levels. It is possible that the lack of marked increase in adrenaline after acrolein exposure might result in differential effects on glucose metabolism than those induced by ozone; however, mechanistic differences regarding how these two pollutants impacts glucose homeostasis and potential contribution of rat strain variations need to be further studied.

In rats, activation of stress response can induce acute adipose lipolysis and muscle protein catabolism leading to increases in circulating medium- and long-chain FFA and BCAA, respectively (Nonogaki, 2000; Porter et al., 2013). We show here that acrolein exposure increased circulating FFA, triglycerides, and cholesterol similar to ozone, but did not increase BCAA, suggesting a potential mechanistic difference from that of ozone. As opposed to ozone, which induces systemic vasodilation and hypothermia (Gordon et al., 2014; Wagner et al., 2014), acrolein exposure increases systemic vasoconstriction in rats at concentrations used in this study (Alarie, 1973). We were unable to determine the core body temperature in this study, but

peripheral vasoconstriction changes are likely associated with core body temperature and metabolism in muscles since it is a major peripheral tissue mass.

Collectively, higher baseline levels of stress hormones, blood glucose, glucose intolerance, and circulating lipids in GK rats relative to Wistars reflects known predisposition of the GK strain to develop nonobese type II diabetes, which is associated with impairment of pancreatic insulin production and secretion (Akash et al., 2013; Beddow and Samuel, 2012). Although the two strains differed significantly in body weight, they were exposed to similar concentrations of acrolein as demonstrated by the minute volume levels normalized to body weight. In spite of GK rats having higher baseline levels of lung injury markers, acrolein-induced neutrophilic inflammation was exacerbated in the metabolically normal Wistar model. This is in contrast to the systemic effects observed following acrolein exposure where hyperglycemia, glucose intolerance, total cholesterol, and FFA levels were further augmented in the GK rats. Exacerbation of these acrolein-induced systemic effects in a diabetic model is consistent with epidemiological evidence pointing to greater vulnerability to air pollutant exposure in those with underlying metabolic disease (O'Neill et al., 2012).

Although this study opens up many different questions about the potential mechanism by which gaseous air pollutants might induce common and distinct systemic and cardiopulmonary responses through differential neuroendocrine regulation, several limitations should be recognized. Since the goal of this study was to produce a measurable systemic response, we used concentrations of acrolein several fold higher than what is normally found in the environment to cause a respiratory reflex reaction. It is likely that at 2 and 4 ppm there was some spillover of acrolein from the nose to the pulmonary airways. We

reasoned that determining the level of injury/inflammation in the nose and lung would permit us to better characterize their relative involvement while using these high concentrations. We did not collectively measure breathing parameters, heart rate, blood pressure, or core body temperature during and post-acrolein exposure, which could further clarify how systemic response is modulated by circulating stress hormones. In addition, we measured acrolein responses in Wistar and GK rats, which might differ from those in the WKY strain that was used for our ozone studies, making direct comparisons difficult. Finally, gender differences were not determined, which are critical since the neuroendocrine stress response and regulation of sex hormones are co-regulated centrally by the hypothalamus.

In conclusion, exposure to the nasal irritant acrolein was associated with prolonged inspiratory and expiratory times indicating labored breathing, induced injury and neutrophilic inflammation in the nasal passages, but caused only an inflammatory response in the lung without increasing vascular leakage. Acrolein elevated corticosterone levels but only slightly increased circulating adrenaline. We also noted that acrolein induced hyperglycemia, glucose intolerance, circulating FAA, and cholesterol levels. Since acrolein is a component of smog and organic combustion processes, the understanding of how it induces neuroendocrine stress response common to other physiological, psychological, and social stressors, and how it modulates respiratory and systemic effects, is important in understanding how environmental exposures are linked to adverse health outcomes in vulnerable populations.

REFERENCES

Akash, M. S., Rehman, K., and Chen, S. (2013). Goto-kakizaki rats: Its suitability as non-obese diabetic animal model for spontaneous type 2 diabetes mellitus. *Curr. Diabetes Rev.* **9**, 387–396.

Alarie, Y. (1973). Sensory irritation by airborne chemicals. *CRC Crit. Rev. Toxicol.* **2**, 299–363.

Bass, V., Gordon, C. J., Jarema, K. A., MacPhail, R. C., Cascio, W. E., Phillips, P. M., Ledbetter, A. D., Schladweiler, M. C., Andrews, D., Miller, D., *et al*. (2013). Ozone induces glucose intolerance and systemic metabolic effects in young and aged brown norway rats. *Toxicol. Appl. Pharmacol.* **273**, 551–560.

Beddow, S. A., and Samuel, V. T. (2012). Fasting hyperglycemia in the goto-kakizaki rat is dependent on corticosterone: A confounding variable in rodent models of type 2 diabetes. *Dis. Model Mech.* **5**, 681–685.

Bosse, Y. (2014). Endocrine regulation of airway contractility is overlooked. *J Endocrinol* **222**, R61–R73.

Chounlamountry, K., Boyer, B., Penalba, V., Francois-Bellan, A. M., Bosler, O., Kessler, J. P., and Strube, C. (2015). Remodeling of glial coverage of glutamatergic synapses in the rat nucleus tractus solitarii after ozone inhalation. *J. Neurochem.* **134**, 857–864.

Conklin, D. J. (2016). Acute cardiopulmonary toxicity of inhaled aldehydes: Role of trpa1. *Ann. N. Y. Acad. Sci.* **1374**, 59–67.

DeJarnett, N., Conklin, D. J., Riggs, D. W., Myers, J. A., O'Toole, T. E., Hamzeh, I., Wagner, S., Chugh, A., Ramos, K. S., Srivastava, S., *et al*. (2014). Acrolein exposure is associated with increased cardiovascular disease risk. *J. Am. Heart Assoc.* **3**(4), e000934.

Delaunois, A., Segura, P., Dessy-Doize, C., Ansay, M., Montano, L. M., Vargas, M. H., and Gustin, P. (1997). Ozone-induced stimulation of pulmonary sympathetic fibers: A protective mechanism against edema. *Toxicol. Appl. Pharmacol.* **147**, 71–82.

Dhabhar, F. S., Malarkey, W. B., Neri, E., and McEwen, B. S. (2012). Stress-induced redistribution of immune cells–from barracks to boulevards to battlefields: A tale of three hormones–curt richter award winner. *Psychoneuroendocrinology* **37**, 1345–1368.

Dorman, D. C., Struve, M. F., Wong, B. A., Marshall, M. W., Gross, E. A., and Willson, G. A. (2008). Respiratory tract responses in male rats following subchronic acrolein inhalation. *Inhal. Toxicol* **20**, 205–216.

Einhorn, I. N. (1975). Physiological and toxicological aspects of smoke produced during the combustion of polymeric materials *Environ. Health Perspect.* **11**, 163–189.

EPA, U. S. (2013). Final report: Integrated science assessment of ozone and related photochemical oxidants. *U.S. Environmental Protection Agency, Washington, D.C.* **EPA/600/R-10/076F**,

Gackiere, F., Saliba, L., Baude, A., Bosler, O., and Strube, C. (2011). Ozone inhalation activates stress-responsive regions of the cns. *J. Neurochem.* **117**, 961–972.

Gordon, C. J., Johnstone, A. F., Aydin, C., Phillips, P. M., MacPhail, R. C., Kodavanti, U. P., Ledbetter, A. D., and Jarema, K. A. (2014). Episodic ozone exposure in adult and senescent brown norway rats: Acute and delayed effect on heart rate, core temperature and motor activity. *Inhal. Toxicol.* **26**, 380–390.

Hamelmann, E., Schwarze, J., Takeda, K., Oshiba, A., Larsen, G. L., Irvin, C. G., and Gelfand, E. W. (1997). Noninvasive measurement of airway responsiveness in allergic mice using barometric plethysmography. *Am. J. Respir. Crit. Care. Med.* **156**, 766–775.

Kodavanti, U. P. (2015). Air pollution and insulin resistance: Do all roads lead to rome?. *Diabetes* **64**, 712–714.

Kodavanti, U. P. (2016). Stretching the stress boundary: Linking air pollution health effects to a neurohormonal stress response. *Biochim. Biophys. Acta.* **1860**(12), 2880–2890.

Lee, B. P., Morton, R. F., and Lee, L. Y. (1992). Acute effects of acrolein on breathing: Role of vagal bronchopulmonary afferents. *J. Appl. Physiol. (1985)* **72**, 1050–1056.

Mazzone, S. B., and Undem, B. J. (2016). Vagal afferent innervation of the airways in health and disease. *Physiol. Rev.* **96**, 975–1024.

Miller, D. B., Ghio, A. J., Karoly, E. D., Bell, L. N., Snow, S. J., Madden, M. C., Soukup, J., Cascio, W. E., Gilmour, M. I., and

Kodavanti, U. P. (2016a). Ozone exposure increases circulating stress hormones and lipid metabolites in humans. *Am. J. Respir. Crit. Care Med.* **193**, 1382–1391.

Miller, D. B., Karoly, E. D., Jones, J. C., Ward, W. O., Vallanat, B. D., Andrews, D. L., Schladweiler, M. C., Snow, S. J., Bass, V. L., Richards, J. E., *et al.* (2015). Inhaled ozone (o3)-induces changes in serum metabolomic and liver transcriptomic profiles in rats. *Toxicol. Appl. Pharmacol.* **286**, 65–79.

Miller, D. B., Snow, S. J., Henriquez, A., Schladweiler, M. C., Ledbetter, A. D., Richards, J. E., Andrews, D. L., and Kodavanti, U. P. (2016b). Systemic metabolic derangement, pulmonary effects, and insulin insufficiency following subchronic ozone exposure in rats. *Toxicol. Appl. Pharmacol.* **306**, 47–57.

Miller, D. B., Snow, S. J., Schladweiler, M. C., Richards, J. E., Ghio, A. J., Ledbetter, A. D., and Kodavanti, U. P. (2016c). Acute ozone-induced pulmonary and systemic metabolic effects are diminished in adrenalectomized rats. *Toxicol. Sci.* **150**, 312–322.

Miller, F. J., Menzel, D. B., and Coffin, D. L. (1978). Similarity between man and laboratory animals in regional pulmonary deposition of ozone. *Environ. Res.* **17**, 84–101.

Moghe, A., Ghare, S., Lamoreau, B., Mohammad, M., Barve, S., McClain, C., and Joshi-Barve, S. (2015). Molecular mechanisms of acrolein toxicity: Relevance to human disease. *Toxicol. Sci.* **143**, 242–255.

Morris, J. B., Stanek, J., and Gianutsos, G. (1999). Sensory nerve-mediated immediate nasal responses to inspired acrolein. *J. Appl. Physiol. (1985)* **87**, 1877–1886.

Munzel, T., Sorensen, M., Gori, T., Schmidt, F. P., Rao, X., Brook, F. R., Chen, L. C., Brook, R. D., and Rajagopalan, S. (2016). Environmental stressors and cardio-metabolic disease: Part ii-mechanistic insights. *Eur. Heart J.* **38**(8), 557–564.

Nonogaki, K. (2000). New insights into sympathetic regulation of glucose and fat metabolism. *Diabetologia* **43**, 533–549.

O'Neill, M. S., Breton, C. V., Devlin, R. B., and Utell, M. J. (2012). Air pollution and health: Emerging information on susceptible populations. *Air Qual. Atmos. Health* **5**, 189–201.

Perez, C. M., Hazari, M. S., Ledbetter, A. D., Haykal-Coates, N., Carll, A. P., Cascio, W. E., Winsett, D. W., Costa, D. L., and Farraj, A. K. (2015). Acrolein inhalation alters arterial blood gases and triggers carotid body-mediated cardiovascular responses in hypertensive rats. *Inhal. Toxicol.* **27**, 54–63.

Porter, C., Hurren, N. M., Herndon, D. N., and Borsheim, E. (2013). Whole body and skeletal muscle protein turnover in recovery from burns. *Int J Burns Trauma* **3**, 9–17.

Snow, S. J., De Vizcaya-Ruiz, A., Osornio-Vargas, A., Thomas, R. F., Schladweiler, M. C., McGee, J., and Kodavanti, U. P. (2014). The effect of composition, size, and solubility on acute pulmonary injury in rats following exposure to mexico city ambient particulate matter samples. *J. Toxicol. Environ. Health A* **77**, 1164–1182.

Snow, S. J., Gordon, C. J., Bass, V. L., Schladweiler, M. C., Ledbetter, A. D., Jarema, K. A., Phillips, P. M., Johnstone, A. F., and Kodavanti, U. P. (2016). Age-related differences in pulmonary effects of acute and subchronic episodic ozone exposures in brown norway rats. *Inhal. Toxicol.* **28**, 313–323.

Soulage, C., Perrin, D., Cottet-Emard, J. M., Pequignot, J., Dalmaz, Y., and Pequignot, J. M. (2004). Central and peripheral changes in catecholamine biosynthesis and turnover in rats after a short period of ozone exposure. *Neurochem. Int.* **45**, 979–986.

Struve, M. F., Wong, V. A., Marshall, M. W., Kimbell, J. S., Schroeter, J. D., and Dorman, D. C. (2008). Nasal uptake of inhaled acrolein in rats. *Inhal Toxicol* **20**, 217–225.

Taylor-Clark, T. E., and Undem, B. J. (2010). Ozone activates airway nerves via the selective stimulation of trpa1 ion channels. *J. Physiol.* **588**, 423–433.

Taylor-Clark, T. E., and Undem, B. J. (2011). Sensing pulmonary oxidative stress by lung vagal afferents. *Respir Physiol. Neurobiol.* **178**, 406–413.

Thiering, E., and Heinrich, J. (2015). Epidemiology of air pollution and diabetes. *Trends Endocrinol. Metab.* **26**, 384–394.

Wagner, J. G., Allen, K., Yang, H. Y., Nan, B., Morishita, M., Mukherjee, B., Dvonch, J. T., Spino, C., Fink, G. D., Rajagopalan, S., *et al.* (2014). Cardiovascular depression in rats exposed to inhaled particulate matter and ozone: Effects of diet-induced metabolic syndrome. *Environ. Health Perspect.* **122**, 27–33.